# Global analyses of cloud fraction and cloud phase by using spaceborne-lidar

*Shuichiro Katagiri[1], Kaori Sato[1], Hajime Okamoto[1]

1. Kyushu University

Information of vertical cloud distribution is crucial for the evaluation of the General Circulation Models (GCMs). There were large varieties in the vertical distribution of low-level clouds sorted by pressure and lower tropospheric stability among the models (Watanabe et al., 2011), while retrieved cloud properties from satellites were not converged. Cesana et al. (2016) evaluated three global cloud phase products using the CALIPSO, and showed large differences among the products. In this study, we revisit cloud detection by space-borne lidar.
We modified our cloud mask algorithm originally developed in Hagihara et al (2010) to increase detectability of optically thick low-level clouds. We use the attenuated total backscattering coefficient at 0.532 $\mu$m for the discrimination the cloudy pixels with the threshold total backscattering coefficient determined by Okamoto et al. (2007) and Okamoto et al. (2008). Remaining noise is estimated by using the data obtained at an altitude of 40 km to avoid contamination of PSCs.
In this algorithm, identification of the fully attenuated pixel is newly introduced. The discrimination confirms whether no cloud is in the atmosphere or no information is received. The fully attenuated mask is determined by referring to whether the surface return can be detectable or not.
After this cloud mask algorithm is applied, we use the cloud phase discrimination algorithm made by Yoshida (2010), which uses the relation between the depolarization ratio at 0.532 $\mu$m and the ratio of two successive attenuated backscattering coefficients at 0.532 $\mu$m in vertical, as proxy of extinction coefficient, to distinguish ice and water particles. Here we rely on the following different scattering properties of water and ice clouds. In case of spaceborne lidar observations, depolarization ratio of water clouds is often comparable to that of ice clouds so that the discrimination between ice and water is not possible by depolarization ratio alone. In turn, water clouds generally show larger extinction coefficients than ice clouds for the same depolarization ratio so that the discrimination become possible by using extinction and depolarization ratio. These characteristics are used in the cloud phase discrimination algorithm.
We will show the global analyses of cloud fraction and water/ice fraction by application of the new cloud mask scheme and differences for the old and new schemes are discussed.

Keywords: cloud, lidar

 

# Studies on horizontal scale, vertical scale, and microphysical properties of convective cloud in tropical Pacific by using Cloud Object analysis method

*Naoya Takahashi[1], Tadahiro Hayasaka[1]

1. Tohoku University

Deep convective cloud is important for modulating climate, radiation budget, and hydrological cycle. In the tropics, the mean radiation budget is significantly affected by the amount of upper-level ice clouds associated with deep convective cloud. The objective of this study is to understand the vertical structure and microphysical characteristics of deep convective clouds. In this study, we used the cloud object analysis method which is introduced in Bacmeister and Stephens (2011). This method evaluates horizontal and vertical scale of cloud by using dataset with active sensors on board satellite. Compared with previous studies, we improved the method by using not only CloudSat satellite but also CALIPSO (Cloud-Aerosol Lidar and Infrared Pathfinder Satellite Observations) satellite. The improved method showed that optically thin cirrus has a significant impact on horizontal and vertical scale of deep convective clouds. Moreover, we took advantages of ice cloud properties retrieval from the CloudSat 2C-ICE product to provide microphysical properties of convective core or anvil part in deep convective cloud. We analyzed only deep convective clouds in tropical Pacific oceans (30˚S-30˚N) and used dataset from 2007 to 2011.

From the comparison horizontal and vertical scale of cloud in western tropical Pacific (WP) and that in eastern tropical Pacific (EP), we found that both horizontal and vertical scale in WP are larger than that in EP. However, ratio of width of convective core to entire horizontal scale of deep convective cloud in WP and EP are almost same. Convective activity in WP and EP are different because of difference in sea surface temperature. It suggested that convective activity has an impact on entire horizontal scale of deep convective clouds.

For evaluation of cloud microphysical properties in the convective core and anvil parts, we investigated vertical distribution of cloud particle effective radius and ice water content in each part. Below 15 km, ice cloud particle effective radius and ice water content of convective core part are larger than that of anvil part. This result seems to reflect the process of formulation of deep convective clouds.

Keywords: Deep convective cloud, Cloud microphysics, CloudSat, CALIPSO

 

# Evaluation of Advantages in GCOM-C Polarization Observation for Estimating Aerosol Optical Thickness

*Risa Miyazaki[1], Hiroshi Murakami[1], Masahiro Hori[1]

1. Japan Aerospace Exploration Agency

GCOM-C (Global Change Observation Mission -Climate) satellite, which is equipped with SGLI (Second generation GLobal Imager) sensor, is planned to be launched in the end of this year. It is designed to conduct optically-based measurements for monitoring global environmental change. The SGLI instrument has three major features: (1) global observation covering wavelengths from 380 nm to 12 μm, (2) 250 m spatial resolution for land and coastal areas, (3) polarization /multidirectional observations and near ultraviolet observation. With these features, GCOM-C will be able to provide many products covering a broad range of topics: land, atmosphere, ocean, and cryosphere. It is especially expected to enable to retrieve land aerosol by polarization (PL: 673.5 and 868.5 nm) and ultraviolet (UV: 380 nm) observations with higher accuracy than by the traditional method using blue and red bands because PL and UV observations have little dependeny on the surface reflectance unlike the traditional one.
In this study, we examined the advantage in the PL and UV observations of SGLI for the estimation of aerosol optical thickness (AOT) over land compared with the traditional method using the radiance at 443 and 673.5 nm.
Our method to evaluate the accuracy of estimated AOT by each method is described below. Monthly AOT and mode radius of aerosol of MODIS L3 products (MYD08_M3) are used as a benchmark. Then, radiance at the top of atmosphere (TOA) is calculated by the results of the radiative transfer model (PSTAR3, [Ohta et al., 2010]) for these input data. The surface reflectances of each wavelength is also estimated by using a month's radiation data of POLDER with the assumption that the minimum of the radiance at 490 nm has information of a clear day. We retrieve the AOT and the mode radius from the radiance of TOA considering the observation accuracy (=SNR) of SGLI and the estimation error of the surface reflectance. In this preliminary work, the aerosol type is fixed as the tropospheric aerosol, which is defined as mixture of a water-solble (0.7) and a dust-like (0.3) aerosol. The accuracy of estimated AOT is evaluated by the deviation from the benchmark AOT. We perform these procedures with both the PL + UV method and the traditional one.
As a results, the accuracy of the estimated AOT improved roughly 10 % by using the method of PL+UV compared the traditional one especially in high surface reflectance areas such as the Sahara desert. This would be because the effect of the estimation error of surface reflectance in the AOT accuracy is considerably large at the high reflectance area. In this presentation, we are going to show the dependency of the estimated AOT accuracy on the geometric condition, the benchmark AOT and its mode radius.

Keywords: GCOM-C, SGLI, Polarization observation, Aerosol optical thickness

 

# satellite view of the widespread haze pollution in China

*Liangfu Chen [1], Minghui Tao [1], Zifeng Wang [1]

1. RADI

*During the last decades, large increase in anthropogenic emissions has led to severe air pollution problems in China, with high concentration of fine particles and widespread haze layers in many areas. The complex sources and high emissions of atmospheric pollutants has exerted great challenge on air quality in China. Compared with regular measurements in ground sites, satellite observations can provide a unique view of the amounts of atmospheric components and formation processes of haze pollution from regional to global scales. Considering the special atmospheric conditions of high aerosol loading and large spatial and temporal variations in China, we made several improvements such as identification of haze areas in the retrieval of aerosol loading. In particular, we conducted comprehensive investigations in optical properties, spatial variation, and formation processes of the regional haze pollution of China using integrated satellite observations, ground measurements, and meteorological data.*

Keywords: air quality , satellite , China

 

# Application of ground observation data in next GSMaP Gauge algorithm

*Tomoaki Mega[1], Tomoo Ushio[1]

1. Graduate School of Engineering, Osaka University

The map of global precipitation amount is one of the important information. The ground-based observation, however, does not cover all Earth. Developed countries operate radar network and rain gauge. Although some developing country installed a few rain gauge or some radars, any developing countries cannot operate radar network and high-density rain gauge network continuously and distribute observation data on time. Observation area of a radar or a rain gauge is local. Development and launching of satellite is expensive. However, characteristic of space-borne observation is to cover whole earth and stable condition.
JAXA is developing and providing near real time global rainfall maps (GSMaP) using the combined Microwave infra-red algorithm with some low orbit satellites. Estimation precipitation by remote sensing of passive microwave radiometer (PMR) is difficult over land. PMR estimation has larger error than ground-based observations. Gauge adjustment GSMaP (GSMaP Gauge) algorithm reduces errors by daily rain gauge. GSMaP Gauge estimated precipitation by precipitation model and daily rain map. Thus quality of GSMaP Gauge depend quality of daily rain map. Available rain gauge map is not uniform quality, because rain-gauges, which real time the map use, are limited number in time.
The plan of the future GSMaP Gauge is to use ground data before the time. The future GSMaP Gauge algorithm uses these data for estimation of the rain model parameters. In no observation area the algorithm interpolate model parameter around ground observation area. The model parameters can improve estimated rain. We will introduce to apply the various ground data in the GSMaP Gauge algorithm.

Keywords: precipitation, satellite

 

# Seasonal and regional dependence of rain estimation from the Himawari-8

*Hitoshi Hirose[1], Atsushi Higuchi[2], Tomoaki Mega[3], Tomoo Ushio[3], Munehisa Yamamoto[1], Shoichi Shige[1], Atsushi Hamada[4]

1. Department of Science, Kyoto University, 2. CEReS, Chiba University, 3. Department of Engineering, Osaka University, 4. AORI, The University of Tokyo

Rain observation with microwave radiometer satellites is essential to make global rain observation data with high temporal resolution. However microwave satellites cannot cover the global area since the number of them is limited. When all microwave satellites are unavailable, utilization of geostationary meteorological satellites (GMS) with high temporal resolution may lead to improvement of rain estimation. Kühnlein et al. (2014) reported that they could estimate rain with high temporal resolution same as GMS by using a statistical method called Random Forest (RF). The machine learning method associates 10 channels information of brightness temperature observed from METEOSAT Second Generation (MSG-2) GMS to rain observation from ground-based radar in Germany. In this method, first some channels are selected randomly from GMS observations to make a small learning sample for rain / no rain classification, called a classification tree. Then the number of tree is increased in the same way, and finally rain / no rain result is classified by majority of all tree' s results. In addition rain type classification and rain rate estimation are possible in the RF method. In previous study, analysis area was limited in Germany due to the limit of ground-based radar observing range, but this study applied the RF method to the third generation GMS, Himawari-8, which can cover the East Asia region widely. Moreover we used precipitation radar of the Global Precipitation Measurement (GPM) main satellite instead of the ground-based radar used by the previous study for the truth of rain. As a result we can estimate rain only from satellite observation and expanding the analysis area to not only mid-latitude region but also tropics.

As compared with Europe region in the previous study, the East Asia region analyzed in this study has various seasonal changes. Therefore this study analyzed seasonal and regional dependence of accuracy in the Himawari-8 –GPM rain product. As a result, accuracy of rain area estimation was higher in JJA including rainy season, and was lower in DJF including snowfall. Accuracy of rain rate estimation was higher in MAM and SON including frontal rain, but was lower in JJA including frequent heavy rain and JDF including snowfall. Moreover we applied the machine learning only in sub-tropic region, and then accuracy of both rain area and rain rate estimation was most high, this result suggested that it was important to limit the learning sample into particular rain system for improvement of rain estimation. In the sub-tropic ocean or summertime land region, Himawari-8 –GPM rain product can detect very smaller rain than a few km scale which is difficult to detect by microwave sensor of the GSMaP. This result shows an advantage of high spatial resolution of the Himawari-8 –GPM rain product.

Himawari-8 GMS data is released from the Center for Environmental Remote Sensing, Chiba University. We used near surface rain observed by GPM (Ku PR) and rain intensity observed by ground-based radar in the Japan Meteorological Agency as the truth of Rain

Keywords: Himawari-8, GPM, machine learning, rain estimation

 

# Variability of Vertical Structure of Precipitation over Sumatra and Adjoining Oceans from Long-Term Measurements of TRMM PR

*Marzuki Marzuki[1], Hiroyuki Hashiguchi[2], Mutya Vonnisa[1], Harmadi Harmadi[1], Ovandriyove Ovandriyove[1], Elfira Saufina[1]

1. Department of Physics, Andalas University, 2. RISH, Kyoto University

This study is a follow-up of a previous study on the vertical structure of precipitation over Sumatra [1]. Spatial, seasonal and diurnal variabilities of the vertical structure of precipitation have been studied using 17 years of Tropical Rainfall Measuring Mission’ s Precipitation Radar (TRMM PR) version 7 data over Sumatra and adjoining oceans. Special emphasis has been put on six different climatic rain regimes, namely, Indian ocean (2 locations), coastal (1 location) and inland (3 locations). The data are classified into different types of precipitation (stratifrom, deep and shallow) including the virga rain. The vertical structure of precipitation over the inland area is compared with long-term measurement of 1.3 GHz Boundary Layer Radar at Kototabang, west Sumatra. The latest TRMM 2A-23 and 2A-25 products (version 7) have been statistically analyzed. First, the spatial, seasonal, and diurnal variations of storm height and freezing level have been investigated. It is found that tall storm is more dominant over the inland than coastal and ocean. Same trend is also observed for melting level height. However, the coastal area has lower percentage of tall melting layer than inland and the ocean. Second, mean vertical profile of radar reflectivity (VPR) has been studied for the stratiform and convective precipitation. The VPR variability has been analyzed for different seasons and diurnal cycles as well as rain intensities. Third, the characteristics of rain intensification and weakening in the vertical direction have been examined by the statistical analysis of VPR gradient (VPRG) above and below the melting layer. Detailed information about the result will be presented during the meeting.

[1] Marzuki, Hashiguchi, H., Kozu, T., Shimomai, T., Shibagaki, Y., Takahashi, Y., 2016, Precipitation Microstructure in Different Madden–Julian Oscillation Phases over Sumatra, Atmospheric Research, Vol. 168, pp. 121-138.

Keywords: vertical structure of precipitation, TRMM PR, Sumatra

 

# Relationships among Vertical Structure of Precipitation, Lightning and Hydrometeor Characteristics along the Equatorial Indonesia

*Marzuki Marzuki[1], Hiroyuki Hashiguchi[2], Mutya Vonnisa[1], Harmadi Harmadi[1], Elfira Saufina[1]

1. Department of Physics, Andalas University, 2. RISH, Kyoto University

In a previous study [1], we have investigated the regional variability of raindrop size distribution (DSD) along the equator through a network of Parsivel disdrometers in Indonesia. Fourth disdrometers were respectively installed at Kototabang (KT; 100.32 E, 0.20 S), Pontianak (PT; 109.37 E, 0.00 S), Manado (MN; 124.92 E, 1.55 N) and Biak (BK; 136.10 E, 1.18 S). We have found that the DSD at PT has more large drops than at the other three sites. The DSDs at the four sites are influenced by both oceanic and continental systems, and majority of the data matched the maritime-like DSD that was reported in a previous study. Continental-like DSDs were somewhat dominant at PT and KT. The differences in the DSD for the four sites may indicate the difference in characteristics of microphysical process accompanying the formation and evolution of DSD at each location which may be related to the variability of topography, mesoscale convective system propagation and horizontal scale of landmass. However, a detailed investigation regarding this hypothesis has not been yet conducted. Therefore, this work tries to overcome such issue by studying the relationship among the vertical structure of precipitation, lightning and the DSD at the fourth locations. The 17 years of latest Tropical Rainfall Measuring Mission’s Precipitation Radar (TRMM PR) (version 7) products are statistically analysed to investigate the characteristics of vertical structure of precipitation at each location. The World Wide Lightning Location Network (WWLLN) data are used to study the lightning characteristics at each location. Detailed information about the result will be presented during the meeting.

[1] Marzuki, M., Hashiguchi, H., Yamamoto, M. K., Mori, S., and Yamanaka, M. D.: Regional variability of raindrop size distribution over Indonesia, Ann. Geophys., 31, 1941-1948, doi:10.5194/angeo-31-1941-2013, 2013.

Keywords: vertical structure of precipitation, Equatorial Indonesia, Raindrop size distribution

 

# Validation of GSMaP using ground snowfall observation data

*Yuki Kaneko[1]

1. Japan Aerospace Exploration Agency

The Global Satellite Mapping of Precipitation (GSMaP) is a global rainfall map based on a blended Microwave-Infrared product and has been developed in Japan for the Global Precipitation Measurement (GPM) mission. GSMaP is the product of an hourly global rainfall map in 0.1-degree latitude/longitude grid and available 3-day after observation through the "JAXA Global Rainfall Watch" web site (http://sharaku.eorc.jaxa.jp/GSMaP).
The latest GSMaP version 04 (algorithm version 07) was released in January 2017 to the public. This product gives snowfall retrieval algorithm for the first time using passive microwave instruments that have higher frequency channels. This algorithm apply the rain/snow discriminant technique developed by Prof. Liu (Sim and Liu 2015, Liu and Seo 2013). The new input data of Multisensor Snow/Ice Cover Maps provided by NOAA/NESDIS make suppress the fake precipitation signals in high latitude area (Kubota et al., in preparation).
This research validates the snow retrieval on GSMaP with the AMeDAS dataset provided by Japan Meteorological Agency(JMA) . The uncertainties of ground observation for snow precipitation amount have been well known. It is often influenced significantly of local climate conditions and small differences in measurement.. JMA mainly uses three types of rain gauge, but those observational errors largely depend on the rain gauge type. Addition to this the effect of the wind is negligible especially for snow observation. WMO suggested the method of double fence interconparison reference (DFIR), but even the DFIR requires the data correction when the wind speed at gauge height is over 6 m/sec.
Thus at first the categorical validation using GSMaP and AMeDAS data and its dependency for the condition such as altitude of the observational site and wind speed. Then the precipitation amount of GSMaP is compared with of on the ground which is corrected by the several methods which suit on the rain gauge types.
The objective of this research is to estimate the accuracy and correlation between the snowfall retrieval from satellite observation and ground measurement.

Keywords: GPM, GSMaP, Solid Precipitation

 

# Estimate performance of Global Satellite Mapping of Precipitation and influence of wind on the performance

*Masato I. Nodzu[1], Jun Matsumoto[1], Long Tuan Trinh[1], Thanh Ngo-Duc[2]

1. Tokyo Metropolitan University, 2. University of Science and Technology of Hanoi

## 1. Introduction

Hanoi urban area, the northern center of Vietnam, is located in the Red River Delta. The growing urban area is faced with the vulnerability by floods. The purpose of this study is to obtain basic knowledge to improve the realtime hydrological forecast system. We examined estimate performance (EP) of Global Satellite Mapping of Precipitation (GSMaP; Aonashi et al. 2009; Ushio et al. 2009) and wind influence on the EP on heavy-rain days.

## 2. Data and Method

We used daily precipitation of GSMaP RNL version 6 in 2001–2007. Vietnam Gridded Precipitation (VnGP; Nguyen-Xuan et al. 2016) was used to validate the GSMaP precipitation as the ground truth. The both data have a resolution of 0.1 degrees. Utilized wind profiles were what operationally observed with rawinsonde at Hanoi. Analyzed months were May, June, July and August with daily precipitation over 3 mm $day^{-1}$ (Nguyen-Le et al. 2015) and dominant westerly winds in the lower troposphere (Nguyen-Le et al. 2014) almost all over North Vietnam at climatology. The 4 months had most of heavy-rain days with precipitation larger than 50 mm $day^{-1}$ over North Vietnam. A rectangle region including the Lo River basin, one of the Red River branch, is chosen as a reference region. We analyzed heavy-rain days with at least one grid over 50 mm $day^{-1}$ in VnGP. GSMaP EP was defined as a ratio of precipitation in GSMaP to that in VnGP for both grid and regional mean precipitation.

## 3. Results

The regional mean precipitation was basically underestimated by GSMaP. Thus, we took a strategy to clarify a reason for underestimate. We defined better and worse estimation (BE and WE) cases as cases with EP from 0.5 to 1.2 and less than 0.5, respectively. Zonal winds were significantly larger in the BE cases than in the WE cases below 500 hPa (Fig. 1). The EP was less than 0.5 in most cases on the days with zonal wind less than 2 m $s^{-1}$ at 700-hPa level (Fig. 2). We compared case-mean EP distribution between the relatively westerly and easterly wind cases (WWC and EWC) at 700-hPa level (Fig. 3). The EP in the WWC was higher over North Vietnam including the reference region than in the EWC (Figs. 3a and b). In the upstream of the Red River, the higher EP region was along the River and the northeastern foot of the Hoang Lien Son Mountains in the WWC (Fig. 3c), while the EP was lower in the southwestern foot. The EP in the WWC is much higher than in the EWC in the downstream of the River. GSMaP even largely overestimated the precipitation in the southward of the Delta. The EP difference between the WWC and the EWC was smaller in the northward than the southward both in the downstream and the upstream. The EP difference was relatively small commonly in the southwestern foor of the mountainous region.

 

## 4. Discussion and Conclusion

These results imply that relatively strong streams made underestimate over the windward region. It is expected that interaction between the topography and winds affected on the EP through the deformation of the hydrometeor distribution on the horizontal-vertical surface. We will investigate the relation between the hydrometeor distribution and the winds in the next step.

References

Aonashi, K., J. Awaka, M. Hirose, T. Kozu, T. Kubota, G. Liu, S. Shige, S. Kida, S. Seto, N. Takahashi, and Y.N. Takayabu, 2009: GSMaP passive microwave precipitation retrieval algorithm: algorithm description and validation. *J. Meteorol. Soc. Japan*, **89A**, 110–136.

Nguyen-Le, D., J. Matsumoto, and T. Ngo-Duc, 2014: Climatologi- cal onset date of summer monsoon in Vietnam. *Int. J. Climatol.*, **34**, 3237–3250, doi:10.1002/joc.3908.

Nguyen-Le D, J. Matsumoto, and T. Ngo-Duc, 2015: Onset of the rainy seasons over the eastern Indochina Peninsula. *J. Climate,* **28**, 5645–5666, doi: 10.1175/JCLI-D-14-00373.1.

Nguyen-Xuan, T., T. Ngo-Duc, H. Kamimera, L. Trinh-Tuan, J. Matsumoto, T. Inoue, and T. Phan-Van, 2016: The Vietnam Gridded Precipitation (VnGP) dataset: Construction and validation. *SOLA*, **12**, 291–296, doi:10.2151/sola.2016-057.

Ushio, T., K. Sasashige, T. Kubota, S. Shige, K. Okamoto, K. Aonashi, T. Inoue, N. Takahashi, T. Iguchi, M. Kachi, R. Oki, T. Morimoto, Z. Kawasaki, 2009: A Kalman filter approach to the Global Satellite Mapping of Precipitation (GSMaP) from combined passive microwave and infrared radiometric data. *J. Meteorol. Soc. Japan*, **87A**, 137–151.

Keywords: Orographic rainfall, Asian monsoon

 

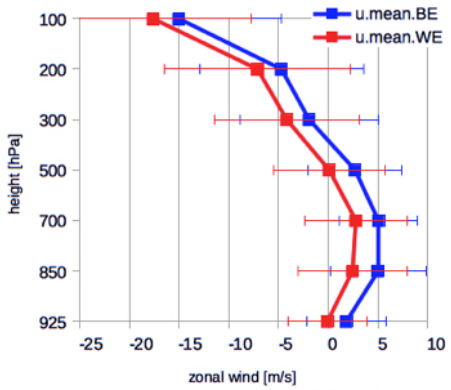


Fig. 1. Mean zonal wind profile in the BE and WE cases in May, Jun, August and September in 2001–2007 at Hanoi.

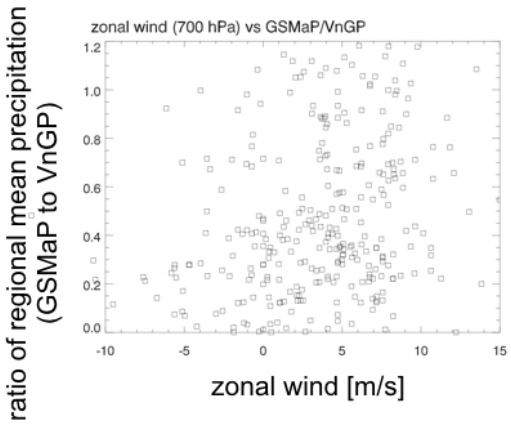


Fig. 2. Relationship between zonal wind at 700 hPa at Hanoi and the estimate performance of regional mean precipitation by GSMaP on heavy-rain days.

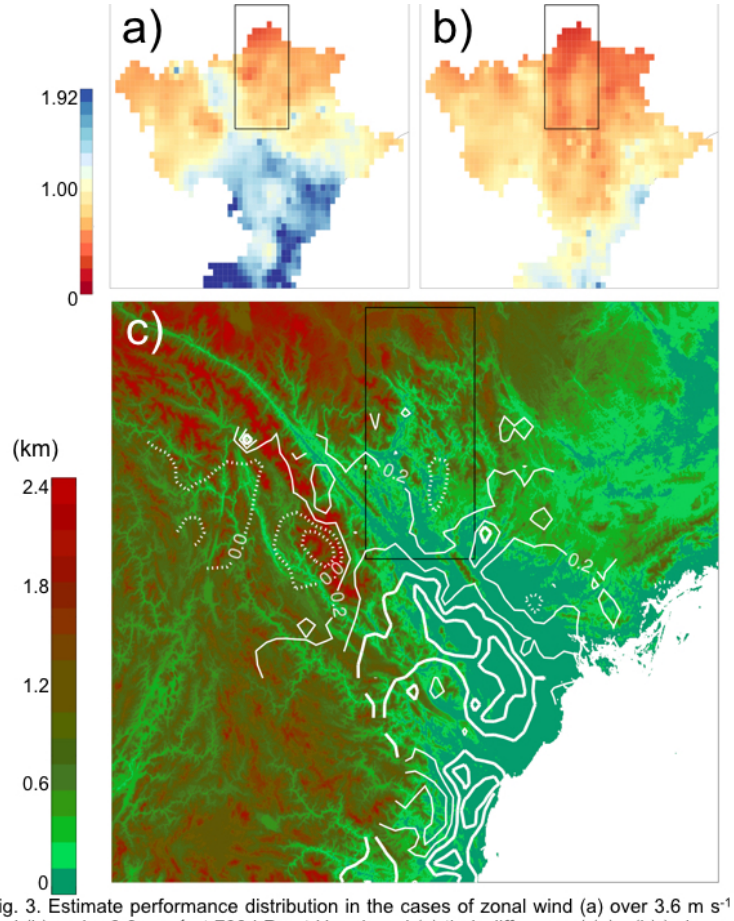


Fig. 3. Estimate performance distribution in the cases of zonal wind (a) over 3.6 m $s^{-1}$ and (b) under 3.6 m $s^{-1}$ at 700 hPa at Hanoi, and (c) their difference ( (a) - (b) ) shown by solid contours (positive values at interval 0.2, starting at 0.2) and dotted contours (negative values at interval 0.2, starting at 0.0) superposed on the topography map.

# Passive microwave rainfall retrievals for tropical cyclones with understanding of microphysical characteristics from cloud resolving models

*Yeji Choi[1], Dong-Bin Shin[1]

1. Yonsei Univ.

Satellite passive microwave observations have been widely used for better precipitation measurements because microwave signals are well associated with the vertically integrated quantities of various hydrometeors in the precipitation system. Understanding the relationships between hydrometeor distributions and radiometric observations is commonly achieved from a-priori information based on cloud and radiation transfer simulations. However, major difficulties in making the a-priori information reside in the simulation variabilities resulted from the assumed microphysical process and insufficient 3-dimensional (3-D) descriptions of radiative signatures as observed by satellite sensors. According to Shin and Kummerow (2003), liquid particle profiles over the precipitation fields can be constructed realistically by matching the radar reflectivity profiles from simulations and GPM dual frequency radar (DPR) observations. However, ice particle profiles produce significant discrepancies in scattering signals depending on the microphysical parameterization methods used in constructing a-priori information. It is then suggested that selecting a proper microphysics scheme showing the most similar microwave signatures for both emission and scattering to the observations can have a substantial impact on the retrieval results. Especially for heavy rainfall systems which can produce large amounts of ice particles, scattering signals should be appropriately described in the a-priori information.
In this study we firstly assessed five microphysical parameterization methods including Thompson, Morrison, WDM6, NSSL-2mom and Thompson aerosol-aware schemes in the Weather Research Forecasting (WRF) model by analyzing the emission and scattering characteristics of each scheme from the perspective of microwave observations for several tropical cyclone cases. Then, the best performed microphysics scheme among them is selected and used to retrieve rain rates. This process may reduce the uncertainties due to the incorrect assumptions on microphysical properties of precipitating clouds. Moreover, as pointed by Kim et al (2016) proper descriptions of the scattering signals along viewing directions can also affect the retrieval quality. We construct more realistic a-priori databases with the 3-D radiative transfer treatment and the best performed microphysics schemes for the GPM microwave imager (GMI). The enhanced prior knowledge is tested to measure the precipitation fields for several tropical cyclone cases.

Keywords: microwave satellite remote sensing, tropical cyclone rainfall measurements, microphysical characteristics of tropical cyclone, microphysics schemes of cloud resolving models

 

# GSMaP RIKEN Nowcast (GSMaP_RNC): an overview

*Shigenori Otsuka[1], Shunji Kotsuki[1], Takemasa Miyoshi[1]

1. RIKEN Advanced Institute for Computational Science

The Japan Aerospace Exploration Agency (JAXA)’s Global Satellite Mapping of Precipitation (GSMaP) provides hourly precipitation estimates over the world except the polar regions. The near-real-time product (GSMaP_NRT) is distributed about four hours after the nominal observation time, whereas the real-time estimate (GSMaP_NOW) is uploaded 30 minutes after the observation time. However, for disaster prevention, short term forecast will add value if available. Otsuka et al. (2016) developed a GSMaP nowcasting system based on space-time extrapolation. The system employs the cross-correlation method to estimate motion vectors of precipitation features, as well as an ensemble Kalman filter to better estimate motion vectors. The system is running stably for more than a year. This year, RIKEN will make the real-time nowcasting products open to public (GSMaP RIKEN Nowcast, GSMaP_RNC). This presentation will provide an overview of the system design and the latest status.

References:
Otsuka, S., S. Kotsuki, and T. Miyoshi, 2016: Wea. Forecasting, 31, 1409-1416.

Keywords: GSMaP, nowcast, data assimilation

 

# Global Drop Size Distribution observed by Dual-frequency Precipitation Radar onboard Global Precipitation Measurement core satellite

*Moeka Yamaji[1], Takuji Kubota[1], Atsushi Hamada[2], Yukari Takayabu[2], Riko Oki[1]

1. Japan Aerospace Exploration Agency , 2. Atmosphere and Ocean Research Institute, the University of Tokyo

Precipitation is one of the most essential parameters in the Earth system. Many places in the world face water problems, such as water shortages and floods. Precipitation observation by rain gauges and ground radars cannot cover overall Earth’ s surface, and are limited spatially and temporally. It is important for us to observe global rainfall by spaceborne sensors.
Following the success of the Tropical Rainfall Measuring Mission (TRMM) launched in 1997, Global Precipitation Measurement (GPM) core satellite was launched in 2014. GPM core satellite carries Dual-frequency Precipitation Radar (DPR), which consists of the Ku-band (13.6GHz) precipitation radar (KuPR) and the Ka-band (35.5GHz) precipitation radar (KaPR). DPR is expected to have better accuracy for precipitation estimation, relative to single-frequency radar (13.8GHz) used in TRMM, by measuring snow and light rain via high-sensitivity observations from the KaPR, and by providing drop size distribution (DSD) information based on the differential scattering properties of the two frequencies. Furthermore, owing to higher orbital inclination of GPM core satellite (65 degrees) than that of TRMM (35 degrees), DPR is the world’ s first space-borne precipitation radar observing middle and higher latitudes area.
GPM/DPR level-2/3 (L2/L3) product provides information of the DSD, which is one of the factors that characterizes precipitation but is a main unknown factor of precipitation remote sensing.
Firstly, we confirm the climatology of particle diameter (Dm, [mm]) and particle number concentration (Nw, [$m^{-3}$]) for 2 years calculated by using GPM/DPR L3 product. Generally, it is found that Dm is larger over land than over the ocean and Nw shows an opposite trend to Dm. In addition, Dm in 20-40 degrees is slightly smaller than other latitudes over the ocean. It is also found that there are seasonal differences in some area, such as Amazon and mid-latitude area. This was consistent with Kozu et al. (2009).
In this study, we use L2 products to analyse in detail by comparing with rain rate. We are planning to apply to the DSD database for Global Satellite Mapping of Precipitation (GSMaP) algorithm in the future.

 

# An experimental study of an Artificial Neural Network (ANN) algorithm to retrieve Precipitable Water (PW) using AHI data

*Yeonjin Lee[1], Myoung-Hwan Ahn[1], Su Jeong Lee[1]

1. Department of Atmospheric Science and Engineering, Ewha Womans University, South Korea

The next Geostationary Korea Multi-Purpose SATellite (GEO-KOMSAT-2A) equipped with the new Advanced Meteorological Imager (AMI), which has improved performance in the spectral (16 spectral bands covering the spectral ranges of 4 visible, 2 near-IR and 10 IR), spatial (2 km at in nadir for the IR channels) and temporal (every 10 min), is scheduled to launch in 2018. It is expected that the finer spatial and temporal distribution of the Total precipitable Water (TPW) product will play an important role in the short-term weather forecast. Current study investigates the possibility of Artificial Neural Network (ANN) approach to retrieve TPW without compensating spatio-temporal resolution of the raw observation data nor the first guess information such as from numerical weather prediction (NWP) model. A multilayer (3 layers; input, hidden and output) perceptron (MLP) feedforward backpropagation algorithm is trained using a training dataset carefully prepared to have general, extensive, and comprehensive representation of real world. The dataset consists of input variables of the simulated Advanced Himawari Imager (AHI) brightness temperatures (9 channels centered at 6.25, 6.95, 7.35, 8.60, 9.63, 10.45, 11.20, 12.35, 13.30 micrometer), 6 dual channel differences, day, time, latitude, longitude, satellite zenith angle and altitude (only land) and the corresponding TPW as output variable. The trained ANN algorithm is applied to the actual AHI data and the results are analyzed to demonstrate the possibility of the ANN TPW for an outbreak of severe convections.

Keywords: Artificial Neural Network, Total Precipitable Water

 

# Development status of the GCOM-W AMSR2 research products

*Nodoka Ono[1], Misako Kachi[1], Takashi Maeda[1], Hiroyuki Tsutsui[1], Mieko Seki[2], Tomoyuki Nomaki[2]

1. Japan Aerospace Exploration Agency, 2. Remote Sensing Technology Center of Japan

The Japan Aerospace Exploration Agency (JAXA) operates the Global Change Observation Mission –Water (GCOM-W) launched in May 2012. The GCOM-W satellite carries the Advanced Microwave Scanning Radiometer-2 (AMSR2). In this mission, eight geophysical values (water vapor, cloud liquid water, precipitation, sea surface temperature, sea surface wind, sea ice concentration, snow depth, and soil moisture) were defined as the standard products, and has been provided to general users since May 2013. Also, research products were defined as a candidate of future standard product in March 2015. Among the standard products, we will update algorithms of sea surface temperature, sea surface wind speed, sea ice concentration, soil moisture content to version 3 in March 2017. As a result of verifying new version products with ground observation and/or other satellite data, accuracy has improved.
For example, regarding the sea surface temperature product, we updated the algorithm to change the method of sea surface wind speed correction and conduct more strict quality check to remove inappropriate buoy data, etc. Then, we calculated the root-mean-square-error (RMSE) between the sea surface temperature by AMSR2 and by buoy data provided by National Oceanic and Atmospheric Administration (NOAA). The verification period is from July 2012 to June 2016. Result shows that the RMSE is 0.52 ℃ in new version and improved while that of previous version is 0.56 ℃. In addition, we update the algorithms of research products that are already open to public, 10 GHz sea surface temperature and all-weather sea surface wind speed, and those accuracies are also improved. At the meeting, we will present the detailed verification results of new version of standard products and research products for AMSR2.

Keywords: satellite remote sensing, Water cycle monitoring, Microwave radiometer

 

# Mean Features of Tropical Cyclone Circulation from QUIKSCAT Sea Surface Wind Observations

*Hirotaka Kamahori[1]

1. Meteorological Research Institute

The mean features of vorticity and divergence fields associated with tropical cyclones are evaluated as anomalies from environmental fields, in six tropical cyclone (TC) active basins (the western North Pacific, the eastern North Pacific, the north Atlantic, the north Indian Ocean, the south Indian Ocean, and the South Pacific), using satellite-derived daily sea surface wind observations. A common feature in all basins is that concentric cyclonic vorticity anomalies extend within a 5-degree radius from the TC center with maximum values of $1.5x10^{-4}$ to $2.0x10^{-4}$ $s^{-1}$. The vorticity field near the TC center is the most intense in the North and the South Indian Ocean, and the weakest in the South Pacific. In terms of horizontal size, the radius at the half maximum ranges from 1.8 to 2.4 degree for vorticity fields with the largest in the South Pacific, and the smallest in the eastern North Pacific. In a case of divergence fields, similar results are found with the largest size in the South Pacific and the smallest in the eastern North Pacific. The cyclonic vorticity anomalies in the inner area are surrounded by anti-cyclonic anomalies in all basins, indicating suppression of convective activity due to the tropical cyclones themselves at a large distance from the center. The anti-cyclonic vorticity have maximum values of around $1x10^{-5}$ $s^{-1}$ and are distributed mainly on the equatorial side of the center. These structures with the cyclonic fields in the inner area and anti-cyclonic fields in the outer area are consistent with the previous study in precipitation fields.

Keywords: Tropical cyclone, Circulation, Sea surface wind

 

# Thermal variability in the South China Sea and its relationship to the western Pacific warm pool

*ChunYi Lin[1]

1. National Museum of Marine Science & Technology

We examine the temperature, heat content, and the size variability in the South China Sea (SCS) connected with the Western Pacific Warm Pool (WPWP), as well as upper-ocean thermal variability in the tropical oceans using satellite data and in situ measurements. Time–frequency–energy distributions, the periods of variability and its trend are extracted by the Empirical Mode Decomposition method and Hilbert–Huang transform method. The increasing rate of mean trend of Western Pacific Warm Pool area is (2.0±0.2) x $10^6$ $km^2$/decade. Furthermore the warm pool area in the SCS has increased by (0.2±0.03) x $10^6$ $km^2$per decade. Observing from the energy of individual component, the semi-annual and annual components forcing from the East Asian monsoon play the main roles on SST variation. Using cross-lag correlation analysis, we demonstrated that the thermal variability in the SCS and WPWP are strongly correlated.

Keywords: South China Sea, Western Pacific warm pool, Thermal variability

 

# Effects of Typhoon and Rainfall on the Kuroshio Surface Temperature and Salinity East of Taiwan

*Chung-Ru Ho[1], Po-Chun Hsu[1], Chen-Chih Lin[1]

1. Department of Marine Environmental Informatics, National Taiwan Ocean University, Keelung, Taiwan

Temperature and salinity are two major variables of the ocean states. Their fluctuations can affect the ocean circulation; moreover, the global changes. In order to understand the effects of wind and rain on the sea surface temperature (SST) and sea surface salinity (SSS) of Kuroshio, we detected the hydrologic characteristics of Kuroshio after heavy rainfall and typhoon passed by east of Taiwan. SST and SSS data are collected from cruises of R/V Ocean Researcher I and spray glider cruises, as well as rain rate data from the Microwave Imager onboard the Tropical Rainfall Measuring Mission. The results show a good correlation between the rain rate and minimum SSS with a coefficient of determination of 0.82 in heavy rainfall cases. The rainfall drops the SSS of Kuroshio with a rain rate of 0.176 psu per mm/hr. Different from the heavy rainfall cases; typhoon not only drops the SST and SSS, but also induces the sub-surface water to uplift. It causes the SSS increases after temporary drops down.

Keywords: Kuroshio, sea surface temperature, sea surface salinity

 

# IoT based visualization service of AMSR2 and GPV in the Arctic Ocean during R/V Mirai cruise MR16-06

*Takeshi Terui[1], Takeshi Sugimura[1], Amane Fujiwara[2], Shigeto Nishino[2], Hironori Yabuki[1]

1. National Institute of Polar Research, 2. Japan Agency for Marine-Earth Science and Technology

Understanding of sea ice situation is the most important issue for vesseles in the sea ice area. In particular, overviewed inforamtion of 1000 km scale is a good indication to determine a safe route. The remote sensing data of sea ice concentration by Earth observation satellites is required. However, limited satelite telecommunication line on the vessel makes on-demand data delivery difficult. And more, if the compressed data would be sent via this line, a professional staff for decoding and visualizing the data must always be needed on the ship. In order to reduce these anxiety and burden, automatical system integrating these processes (delivery, decoding, and visualizing data) is needed. ADS (Arctic Data archive System) has been developed the new integrated system for the ship to delivery and visualize data, which is called VENUS (VEssele Navigator by Unitized Systems). This system was implemented to R/V Mirai cruise MR16-06. In this research, we want to introduce technical performances and advantages of this system.

Keywords: IoT, Raspberry Pi, AMSR2, Ship, Visualization, Automation

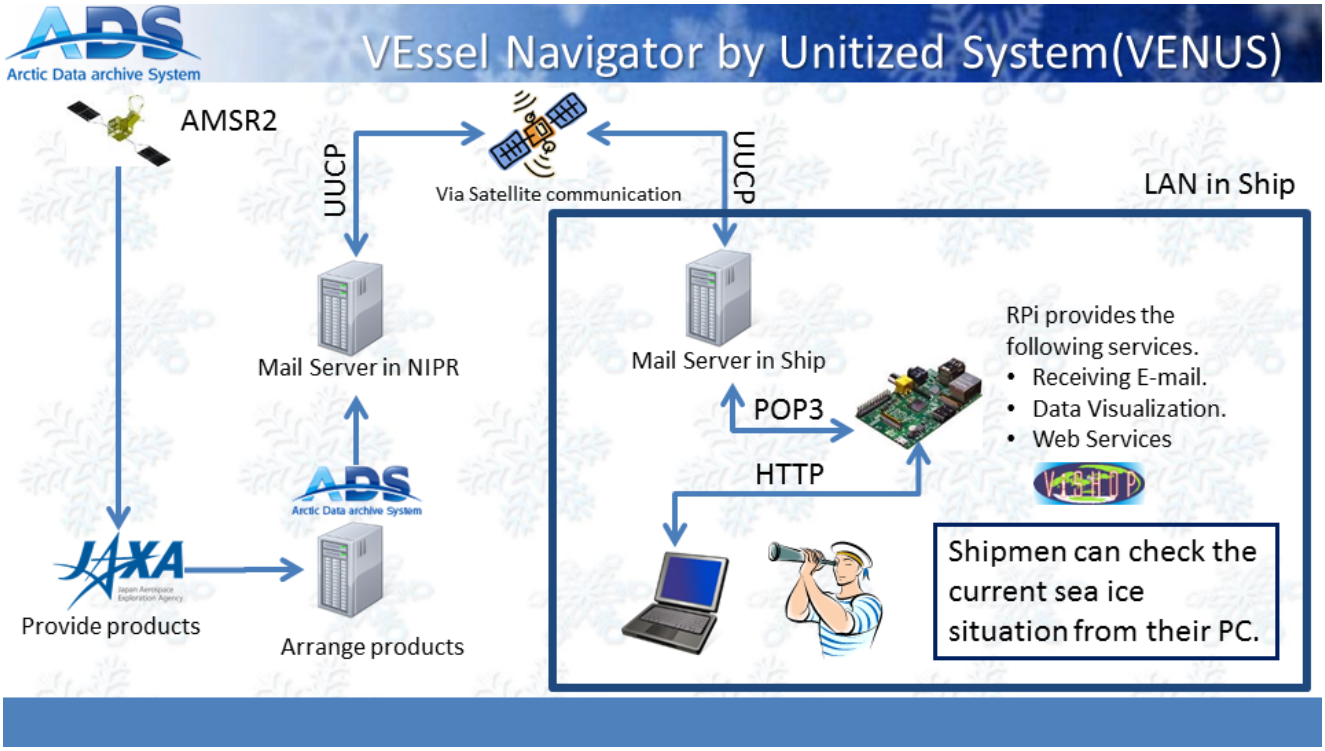


 

# Development of Arctic Route Search System on ADS

*Takeshi Sugimura[1], Takeshi Terui[1], Hironori Yabuki[1], Hajime Yamaguchi[2]

1. National Institute of Polar Research, 2. University of Tokyo

The aim of this study is to build the Arctic Route Search System in order for everyone can easily search optimum navigation route. This system is constructed on ADS (Arctic Data archive System) based on the research products by Arctic Sea Route research group (Yamaguchi laboratory in the University of Tokyo) in ArCS project. In this application, we estimate a sea ice situation and a navigational difficulty from Ice Index based on sea ice concentration and sea ice thickness. A* search algorithm is adopted as search algorithm which select a route with smallest navigation cost among the possible route.
In the present system, because AMSR2 satellite data is used as input condition, route prediction cannot be performed. We are improving the system to use sea ice forecast model TOPAZ4 dataset for input condition, and expect to predict a navigation route for a time period up to 10 days.

Keywords: Northern Sea Route, ADS, AMSR2, TOPAZ4

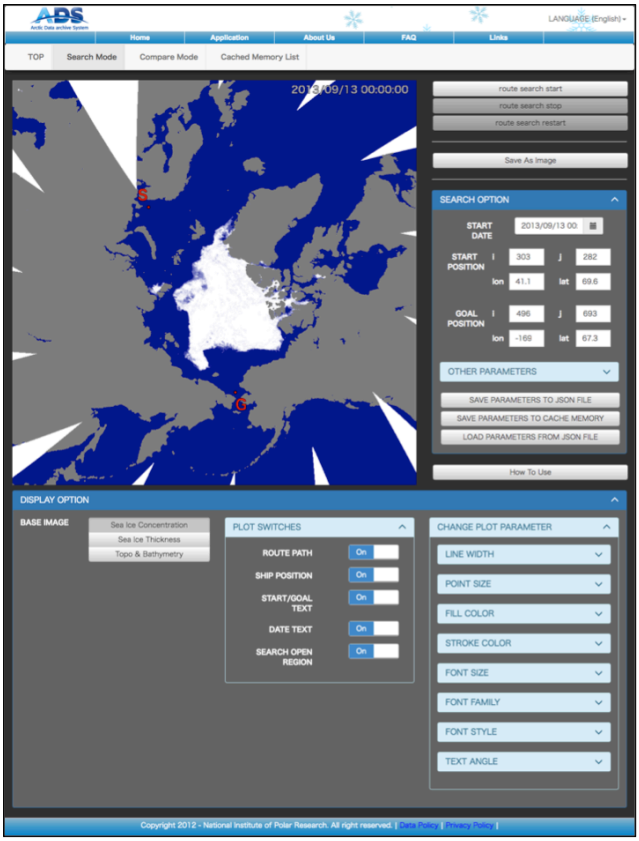


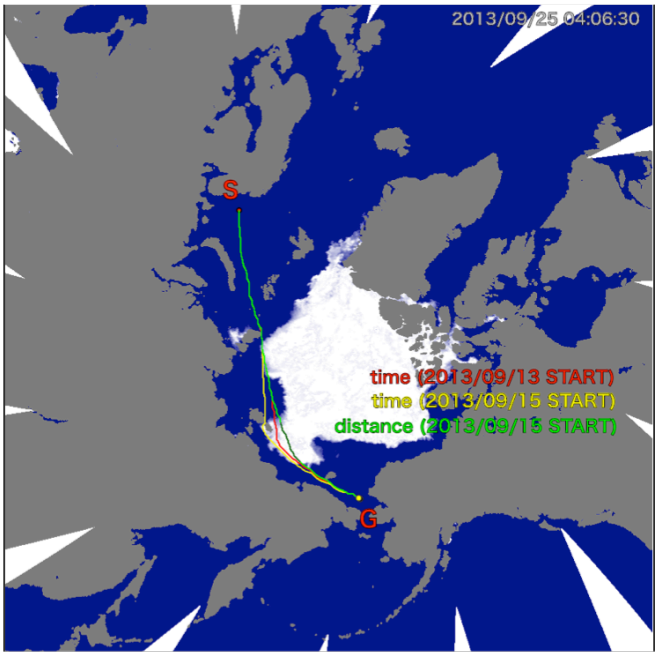


 

# Influence of the sea-ice and cloudiness on the reflectivity over the Southern Ocean

*Alessandro Damiani[1], Raul R. Cordero[2]

1. Chiba University, 2. Santiago de Chile University

The influence of the cloud cover and sea ice concentration (SIC) on the Ultraviolet (UV) Lambertian equivalent reflectivity (LER) at the top of atmosphere over the Southern Ocean has been evaluated for the 1979-2012 period. Despite the high cloud fraction for most of this period, the influence of sea ice was found to be larger than that of cloud cover and it was the main driver of the reflectivity variability. Overall, an increment of the SIC from 0% to 100% resulted in a LER increase of 44 reflectivity units. This value is about twice of the corresponding sea ice-induced reflectivity increase calculated for the observed and modeled shortwave albedo, which is the variable of interest for climate change. On the other hand, cloudiness was found to enhance the UV-LER mostly for low SIC levels. Nevertheless, the analysis was constrained by the difficulty of the passive satellite instruments in identifying cloudiness over high SIC and by the short time series from additional active sensors. Overall, the distribution of the reflectivity for different regions and months shows a marked seasonal-dependent double peak. The reflectivity of the grid-cells characterized by a SIC larger than 30% showed statistically significant negative trends in particularly for the Bellingshausen/Amundsen sea sector. In contrast, the trend of the ice-free grid-cells of the whole Southern Ocean was generally positive.

Keywords: reflectivity, Antarctica, sea ice, cloud fraction

 

# Analyzing Variations of the Kuroshio east of Taiwan using Satellite Altimetry and Hydrographical and Tide gauge data

*Wen-hau Lan[1], Chung-Yen Kuo[1], Chi-Hung Chang[2], C.K. Shum[3], Yuchan Yi[3]

1. Department of Geomatics, National Cheng Kung University, Tainan, Taiwan, 2. Geosensing Systems Engineering and Sciences, University of Houston, Texas, USA, 3. Division of Geodetic Science, School of Earth Sciences, Ohio State University, Ohio, USA

Kuroshio is one of the major currents in the world and plays an important role in the North Pacific climate system due to the sea water, heat and salinity transport and complex air-sea interaction, which is also strongly related to local climate stabilization and natural hazard. In recent years, the velocity of Kuroshio Current increases, attributing to the changes in wind stress over the North Pacific under global warming and affecting sea level along the eastern coast of Taiwan and northward heat transport. Therefore, monitoring of the Kuroshio is of scientific and practical importance. In the study, we focus on the use of contemporary multi-mission satellite radar altimetry and *in-situ* MBT/XBT/Argo to calculate the surface and subsurface (0-2000 *m*) geostrophic velocities and the transport of the Kuroshio east of Taiwan based on the geostrophic balance equation. In addition, we will also analyze interannual and seasonal variations of the Kuroshio transport east of Taiwan using long-term tide gauge data. The estimated current velocities are validated using *in situ* mooring drifters or Argo drift trajectories, and used to study the evolution of the Kuroshio east of Taiwan and the correlation with climate indices, such as the Multivariate ENSO Index (MEI) and the Pacific Decadal Oscillation (PDO) index.

Keywords: Kuroshio Current, Satellite Altimetry , Tide gauge

 

# Improvement of Multi-Altimeter Data by Waveform Classification and Retracking: A case study of Taiwan’ s wetland

*Wei-Ming Chuang[1], Huan-Chin Kao[1], Chung-Yen Kuo[1], Kuo-Hsin Tseng[2], C. K. Shum[3], Ting-Yi Yang[3]

1. National Cheng Kung University, Taiwan, 2. National Central University, Taiwan, 3. Ohio State University, USA

Satellite radar altimetry becomes an irreplaceable tool to provide accurate surface height measurements over open oceans. However, the accuracy decreases when altimeters approach coastlines or non-ocean surfaces due to the improper geophysical corrections and complex returned waveforms. Many algorithms have been developed for waveform retracking that can improve the accuracy of altimetry data; however, the performance still cannot achieve the same accuracy as that in open oceans. In coastal regions, some waveforms reflected from non-ocean surfaces lead to the worse retracking results. Therefore, waveform classification methods are needed to distinguish waveforms which is truly reflected from ocean or not. Waveform classification used in this study includes two steps. The first step is applying Principal Components Analysis (PCA) to waveforms to extract the features for classification. The second step is using Density-Based Spatial Clustering of Applications with Noise (DBSCAN) to separate waveforms into two groups: ocean and non-ocean waveforms. Then, we remove the non-ocean waveform to improve the accuracy before doing retracking. In this study, we use Jason-2, Envisat and Altika altimetry data over Hsiang-Shan wetland, which is located in Northwestern Taiwan. The satellite-derived results are then evaluated using Hsin-Chu tide gauge data. Finally, we expect building an effective classification method and figuring out the most appropriate retracking algorithm applied for this study area.

Keywords: coastal altimetry, waveform classification, waveform retracking, Hsiang-Shan wetland

 

# The Relationship between the Sea Surface Temperature and Chlorophyll-a in the Global Ocean

*fengchun Su[1], Yung Shiang Lee[2], ChunYi Lin[1]

1. National Museum of Marine Science & Technology, 2. Department of Wealth Management, Hsing-Wu University

The sea surface temperature (SST) and sea surface chlorophyll-a (Chl-a) play important roles in the primary production. However, it is unclear between SST and Chl-a in the ocean. In this study, SST and Chl-a derived from NASA (National Aeronautics and Space Administration) /MODIS (MODerate Resolution Imaging Spectro-radiometer) sensor are gathered from 2001 to 2007. The missing data of SST and Chl-a are filled up by the Data Interpolating Empirical Orthogonal Functions (DINEOF) method. The correlation between SST and Chl-a time series data for each grid is examined. So that a correlation map over the entire global ocean can be constructed to see whether there exists any regional dependence. The results suggest the place of ocean currents and ocean gyres play an important factor between SST and Chl-a. It is found that higher positive correlation area of SST and Chl-a time series is located in most coastal ocean area and where the ocean current flow through. The correlation between the two time series is typically negative correlation in most gyres of ocean. This information could be useful for the study of global changes in sea surface temperature and marine biosphere.

Keywords: Sea Surface Temperature, Sea Surface Chlorophyll-a, Remote-Sensing

 

# The method deriving sea surface temperature - an empirical study on geostationary meteorogical Himawari-8 satellite.

*Yung Shiang Lee[1], ChunYi Lin[2], YuMei Yeh[1], fengchun Su[2], Yu-Hsin Cheng[3]

1. Hsing Wu University, Taiwan, R.O.C., 2. National Museum of Marine Science & Technology , Taiwan, R.O.C., 3. State Key Laboratory of Marine Environmental Science, College of Ocean and Earth Sciences, Xiamen University, Xiamen, China

Sun-synchronous satellites significantly better than geostationary satellites at a time resolution. Recent studies sea surface temperature (SST) mostly as a reference material Moderate Resolution Imaging Spectroradiometer (MODIS). The equatorial region of the tropical Pacific SST bias main factors are wind speed and latent heat in past studies. In this study, deriving the SST in the equatorial region of the western tropical Pacific. Using information from geostationary meteorogical Himawari-8, which data products are level 0. The time span of the data is from July 2015 to December 2016. We apply and compare data mining techniques to improve the quality of Himawari-8 SST. In past study, by a logistic regression approach, it can be determined with an accuracy of 0.4$^{o}$K and an improvement of the correction to 95%.

Keywords: Sea Surface Temperature, tropical Pacific, Wind speed, latent heat

 

# Spatiotemporal variation of vegetation index and sun-induced fluorescence depending on temperature conditions in the Korean peninsula.

*Jae-Hyun Ryu[1], Dohyeok Oh[1], Jaeil Cho[1]

1. Chonnam National University

Current anomalous climate by climate change could cause critical problems in ecology and society. Drought by water deficit and heatwave has been occurred frequently in the Korean peninsula over recent years. Under those abnormal conditions, crop and forest suffered from water and heat stress and they will lead to the decline of crop yield and the weaken ecosystem service. The satellite remote sensing has been applied to monitor the change of vegetation health according to drought event using vegetation indices such as the normalized difference vegetation index (NDVI). Sun-induced fluorescence (SIF) as well as vegetation indices also could indicate the degree of vegetation stress. In this study, the aim is to evaluate the spatiotemporal variations of NDVI and SIF depending on temperature conditions using satellite data in the Korean peninsula. The NDVI from Aqua/Moderate Resolution Imaging Spectroradiometer (MODIS) and the SIF from Meteorological Operational Satellite-A (MetOp-A)/Global Ozone Monitoring Experiment-2 (GOME-2) were used from 2007 to 2016 that these periods include severe drought years. In addition, the MODIS land surface temperature (LST) was used to represent the temperature condition. The seasonal variations of NDVI and SIF were changed according to the degree of drought events, particularly SIF in spring. Also, the value of SIF on August 2016 was dropped comparing the other years due to the critical physiological stress by the worst recorded heat wave. In addition, the increased patterns of SIF or NDVI to LST was clearly shown under the condition less than about 29˚C, and both SIF and NDVI were decreased at higher temperature condition. However, the sensitivities of NDVI or SIF to LST was higher in crop than forest. Further, depending on the regions, South and North Korea, the patterns of NDVI or SIF to LST was different: The forest in North Korea were more sensitively responded than South Korea. Our results represented that NDVI and SIF were useful indicators to detect the heat stress on vegetation and to understand effect of climate.

Keywords: Vegetation index, Sun-induced fluorescence, Temperature, Korean peninsula

 

# Retrieving solar-induced chlorophyll fluorescence from GOSAT measurements with considering radiance offset's dependence on solar zenith angle and observed radiance

*Haruki Oshio[1], Yukio Yoshida[1], Tsuneo Matsunaga[1]

1. National Institute for Environmental Studies

In recent years, satellite remote sensing of solar-induced chlorophyll fluorescence (SIF) has attracted attention as a method for elucidating the photosynthetic activity of terrestrial vegetation. SIF is emitted by chlorophyll molecules: part of the solar radiation absorbed by chlorophyll is not used for photosynthesis and re-emitted as red and far-red radiation. SIF includes information on partitioning of the absorbed solar radiation by chlorophyll. Several studies retrieved SIF from high-resolution spectra in far-red domain obtained by the greenhouse gases observing satellite (GOSAT). The retrieval principle was based on the filling-in of Fraunhofer line by SIF. Non-linearity of the analog circuit in GOSAT spectrometer adds indistinguishable zero-level offset term to SIF. Therefore, the zero-level offset correction becomes important to obtain the SIF accurately.
The zero-level offset can be evaluated from the retrieved filling-in signal (= zero-level offset + SIF) over the vegetation-free areas where the value of SIF is expected to be zero. Previous studies showed that the zero-level offset increases according to the increase of observed radiance. We investigated the zero-level offset for different land covers and locations and found that the zero-level offset relies not only on the observed radiance but also on the solar zenith angle (SZA). Even when the observed radiance was same, the zero-level offset increased according to the decrease of SZA. Therefore, 2-D correction table considering the observed radiance and SZA was prepared for the zero-level offset correction.
Monthly variation of SIF corrected by the present method was compared with that corrected by the previous method. The comparison was conducted for central Africa (woody savanna), southeast USA (evergreen needle leaf), and west Europe (grassland and cropland). The difference was largest for central Africa and smallest for west Europe for almost all month. The maximum difference reached 0.23 and 0.15 $mW/m^2 \cdot sr \cdot nm$ for central Africa and west Europe, respectively. Typical monthly averaged SIF ranged 0–1.5 $mW/m^2 \cdot sr \cdot nm$, thus the difference is significant. Furthermore, the difference was largest in summer for southeast USA and west Europe and in spring for central Africa. This study highlights that indispensable attention is required when the value of SIF is directly used and seasonal cycle is compared among locations having different surface cover and latitude.

Keywords: solar-induced chlorophyll fluorescence, GOSAT, photosynthetic production

 

# Satellite observation of internal waves converting polarity in the South China Sea

*Chan Zhang[1]

1. Second Institute of Oceanography, State Oceanic Administration

According to Synthetic Aperture Radar (SAR) imaging mechanism, the oceanic internal solitary waves (ISWs) can be well recognized. In this study, the polarity conversion of ISWs in the South China Sea (SCS) is investigated using 10-years SAR images from 1999 to 2009. It is found that most of the ISWs in SCS are the depression ISWs. However, in region of the continental shelf of the SCS, some elevations ISWs can be identified. In the total of the 500 oceanic internal wave SAR images used in this study, 32 of them exhibit oceanic internal wave polarity conversion.
Moreover, it is found that the elevation ISWs do not show seasonal-locking characteristic. ISWs are found nearly in every season. The bottom topography, hydrological conditions and local thermocline structure which are generally regarded as the conditions for the generation of the elevation ISWs are further explored. Taking the two-layer KdV theory, it is found that ISWs in SCS exhibit a time gap of about 12.4 hours. This time gap is well consistent with the period of local semi-diurnal tide. Our findings thus strongly suggest that the elevation ISWs in SCS can be evolved from the depression ISWs in SCS, which are generally originated from Luzon strait.

Keywords: oceanic internal solitary waves, polarity conversion, depression ISWs

 

# Uncertainty Estimation of Soil Moisture Datasets Using Triple Collocation Methods at Mongolian Grassland

Kohei Suzuki[2], *Jun Asanuma[1], Ichirow Kaihotu[3]

1. Center for Isotopes and Environmental Dynamics, University of Tsukuba, 2. Graduate School of Life and Geoenvironmental Sciences, 3. Graduate School of Integrated Arts and Sciences, Hiroshima University

Uncertainties in soil moisture (SM) datasets were estimated at semi-arid grassland in Mongolia by applying the triple collocation methods (TC). Three SM datasets applied to TC are a SM product of AMSR-E, GLDAS with Noah, and the in-situ measurements.
First, in order to demonstrate capability of TC, the uncertainties acquired through TC and a statistical measure are compared. The results showed that the TC uncertainties of AMSR-E are found to be smaller than the root mean squared difference (RMSD) between AMSR-E and the in-situ measurements. This indicates that the latter includes the systematic errors as well as the random errors of AMSR-E and the in-situ, while the TC uncertainties only identifies the random error of AMSR-E. Therefore, it was shown that TC is capable of providing an absolute measure of uncertainties in a SM dataset, unlike other statistical measures such as RMSD.
Further analyses showed that differences of the vegetation amounts expressed in NDVI and difference between ascending/descending observations of AMSR-E do not cause significant difference in the magnitude of uncertainties. This suggests that these factors did not influence uncertainties of AMSR-E.
It is also discovered that, in a few cases, TC cannot calculate uncertainties, which may be attributed to a violation of some of the TC assumptions. This is consistent with previous claims that TC is vulnerable to violations of the assumptions. The current findings suggest that the proper selections and pre-processing of the datasets are of significance.

Keywords: Soil Moisture, Satelite Remote Sensing, AMSR-E, Satellite products validation

 

# Downscaling of AMSR2 soil moisture content using multi-satellite land surface variables with regression kriging

*DAEYUN SHIN[1], Daesun Kim[2], Nari Kim[2], Yangwon Lee[2], sunghwa choi[1]

1. KWCI , 2. Pukyong National University

Soil moisture is a primary state variable of hydrology and the water cycle over land. Recent remote sensing technologies have enabled microwave satellite sensors to monitor soil moisture for wide area irrespective of weather conditions. AMSR-E (Advanced Microwave Scanning Radiometer - Earth Observing System) instrument on board the Aqua satellite which was launched in 2002 provided global daily 25-km soil moisture data, and MIRAS (Microwave Imaging Radiometer with Aperture Synthesis) instrument on board the SMOS (Soil Moisture and Ocean Salinity) satellite which was launched in 2009 produces global daily 25-km soil moisture data. Also, AMSR2 (Advanced Microwave Scanning Radiometer 2) instrument on board the GCOM-W1 (Global Change Observation Mission-Water 1) satellite which was launched in 2012 succeeds the role of AMSR-E and provides global daily 25-km and 10-km data. NASA (National Aeronautics and Space Administration) has launched SMAP (Soil Moisture Active Passive) satellite in 2015. It has an active radar and a passive radiometer for producing global daily 3-km and 36-km soil moisture data, respectively, but owing to the failure of the radar, only 36-km data is available now. The spatial resolution of 10 to 36 km is not sufficient for regional-scale applications for hydrology and meteorology although the temporal resolution is quite appropriate. To solve the problem of limited spatial resolution of soil moisture data retrieved from microwave satellite sensors, this study presents the downscaling by spatial statistical methods combined with various land surface variables. To date, statistical methods such as multiple regression and machine learning have been employed for downscaling of soil moisture. However, the inevitable residuals (that is, the part which cannot be explained by the statistical models) bring about differences between the original and the downscaled data, so the consistencies between them may not be maintained. To overcome the drawback, a novel method named regression kriging has been proposed by combining multiple regression and kriging interpolation. Downscaling by the regression kriging can produce a high-resolution data which is spatially consistent with the original data through the correction of residuals. Several studies conducted the downscaling by regression kriging for rainfall datasets such as TRMM (Tropical Rainfall Measuring Mission), but the application of this novel method to soil moisture dataset has not been reported yet. In this study, we carried out the downscaling of AMSR2 soil moisture data using multi-satellite land surface variables with the regression kriging. The database for LST (land surface temperature), RR (rising rate of LST in daytime), NDVI (normalized difference vegetation index), NDWI (normalized difference water index), TVDI (temperature vegetation dryness index), and SA (surface albedo) was built using the satellite images from MODIS (Moderate Resolution Imaging Spectroradiometer) and COMS (Communication, Ocean and Meteorological Satellite). The low-resolution soil moisture data from AMSR2 on the 10-km grid was downscaled on the 1-km grid using the land surface variables. The spatial consistency before and after downscaling was be measured by comparing the pixel values of the low-resolution grid with the upscaled block means of the high-resolution grid. Our results of the spatial consistency showed a correlation coefficient greater than 0.95. The downscaled soil moisture data can be used in various regional-scale applications for hydrology and meteorology.

Keywords: Satellite remote sensing , Soil moisture, Statistical downscaling, Regression kring

 

# The nonlinear three-band algorithm for retrieving land surface temperature from Himawari-8

*Yuhei Yamamoto[1], Hirohiko Ishikawa[1]

1. Disaster Prevention Research Institute, Kyoto University

## Introduction

The land surface temperature (LST) is a key parameter of the land-atmosphere interaction on various scales. Since satellite observations can provide LST data over wide area in homogeneous quality, LST retrieval algorithms have been proposed for various sensors. The Advanced Himawari Imager (AHI) onboard Himawari-8, a next-generation geostationary satellite, has three thermal infrared bands in the spectral range 10–12.5 $\mu$m, while previous satellites had two. The 10–12.5 $\mu$m range is suitable for retrieving LST since the atmospheric absorption is small in this range, and is mainly by water vapor. Another advantage of this range is that the land surface emissivity (LSE) does not differ much among various constituents of the land surface. The retrieval of the LST is sensitive to LSE estimation and water vapor estimation. (Li et al., 2013). Therefore, a retrieval algorithm that has high accuracy and high robustness against the uncertainties in input data is required. We present a new LST retrieval algorithm that makes the maximum use of AHI new window thermal infrared (TIR) bands.

## Method

Previous studies (Atitar and Sobrino, 2009; Takeuchi et al., 2012) employed a nonlinear split-window algorithm (NSW), which considers the effect of the atmospheric attenuation by utilizing the differential adsorption of two adjacent TIR bands. In contrast, we have developed a nonlinear three-band algorithm (NTB) by utilizing a combination of AHI three TIR bands. The NTB is inspired from a three-band algorithm (TB) developed by Sun and Pinker (2003) which used two TIR and a near infrared band. The formula of the algorithm includes ten coefficients. The optimum values of these coefficients are derived using a statistical regression method from the simulated data, as obtained by a radiative-transfer model. The simulated data sets include the spectral response functions for the three AHI TIR bands, the seven satellite zenith angles (SZAs) from 0˚ to 60˚, 215 radiosonde profiles, 6 LSTs for each profile, and 86 band LSEs. As a result, 109467 LST –($T_{10.4}$, $T_{11.2}$, $T_{12.4}$) relations were obtained in total for a fixed SZA value. After obtaining the coefficients in this way, we searched the best LST algorithm for five cases: three types of NSWs, one type of TB and one type of NTB.

## Results

We checked the root-mean-square error (RMSE) in terms of the SZA, LST and precipitable water (PW) dependence by using dataset used to obtain coefficients. The result showed that the NTB can stably estimate the LST especially in hot and wet environments by comparison to the NSW. Moreover, we evaluated the sensitivities of five LST algorithms to the uncertainties in LSE, PW and noise equivalent delta-temperature (NEdT) by using the validation data independent of dataset used to obtain coefficients. Consequently, it was clarified that the NTB has the highest robustness against the uncertainties in LSEs and NEdTs of three TIR bands. The total estimation error of NTB is about two third of NSW for SZA smaller than 40˚. Therefore, it is concluded that the NTB is more suitable for the LST retrieval from AHI than the NSW.

The NTB is combined with an appropriate cloud mask and a LSE products to retrieve LST (see Figure 1 for example). The spatial resolution of the AHI is about 2 km and the observation cycle is 10 minutes. Though the horizontal resolution is inferior to the products from polar-orbiting satellites, the high frequency

 

observation explores new use of LST products. For example, the AHI can detect a difference in urban area such as commercial, industrial, and residential regions. Hence, it is expected that our Himawari-8 LST product is applicable to studies of thermal property in smaller scales (see Figure 2).

**References**

Z. Li *et al.*, *Remote Sens. Environ.*, vol. 131, pp. 14–37, 2013.
M. Atitar and J. A. Sobrino, *IEEE Geosci. Remote Sens. Lett.*, vol. 6, no. 1, pp. 122–126, 2009.
W. Takeuchi *et al.*, *Asian J. Geoinformatics*, vol. 12, no. 2, 2012.

Keywords: Land surface temperature (LST), Himawari-8, Remote sensing

 

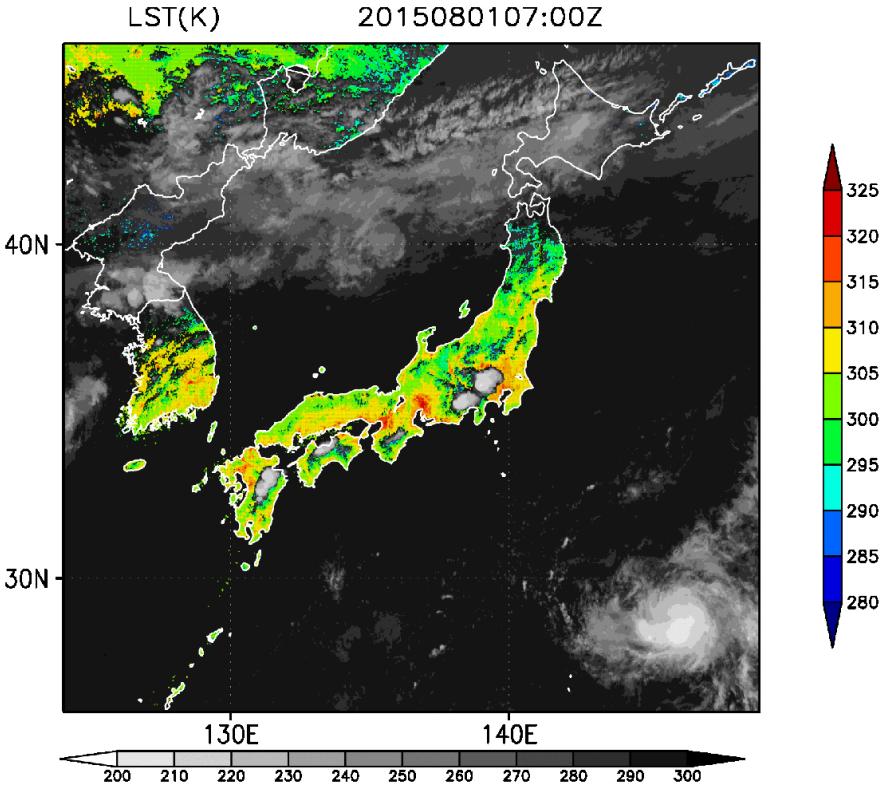


Figure 1. An example of the Himawari-8 LST product over Japan area on 01 August 2015 at 07:00 UTC.

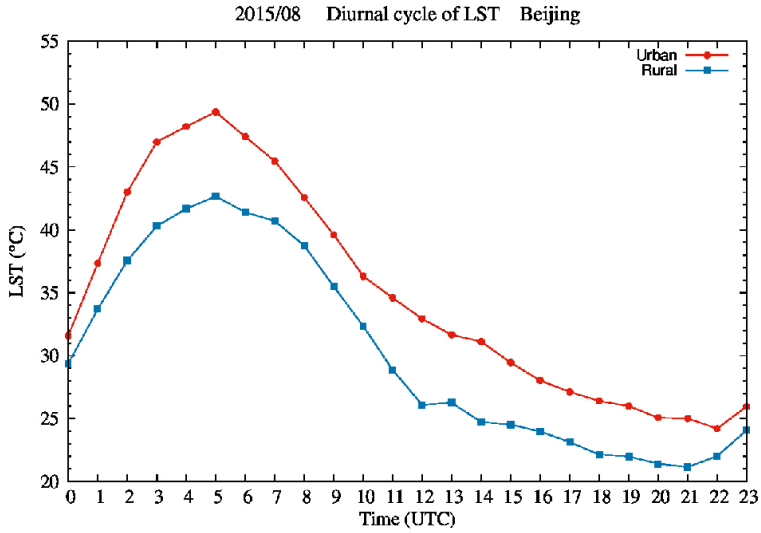


Figure 2. The Diurnal cycle of LST in Beijing urban and rural areas which was generated by composite processing for 31 days in August 2015. The temporal resolution was reduced to 1 hour.

# A dynamic approach to retrieving snow depth based on the technology of integrating satellite remote sensing and in situ data

*Liang Zhao[1,2], Yuxiang Zhu[3], Ziniu Xiao[1]

1. LASG, Institute of Atmospheric Physics, Chinese Academy of Sciences, 2. National Climate Center, China Meteorological Administration, 3. CMA Training Center, China Meteorological Administration

Hydrological processes and climate in the extratropics are highly affected by the seasonal snow. Essential characteristics both for hydrology and climatology include snow water equivalent and snow depth. We develop a new approach to dynamically retrieving snow depth based on integration of passive microwave remote sensing and in situ data. First, the snow-cover confidence index is established by use of both the passive microwave remote sensing and in situ data, identifying together the snow cover; second, a new dynamic parameterized scheme (distance weighted method) is developed based on the index. The characteristics of the snow-depth retrieval approach are following: on the one hand, for the difference issue of retrieval coefficients in different spatial-temporal circumstances, a solution is proposed that retrieval coefficients are adjusted according to real-time observed snow depth, being the biggest difference from static retrieval approaches; on the other hand, the advantage of spatial-temporal continuity of the passive microwave remote sensing data has been exploited, being able to retrieving the snow depth with relative high resolution and precision in the west China where few stations are located. The results show that the approach implements the efficient integration of passive microwave remote sensing and observed data, exerts the advantages of different source data, improves obviously the retrieval precision in the west China and the south marginal regions of snow cover in the east China, and solves the question in the old integrating approach that the area of snow cover was always relatively smaller in the west China, amplifying the detectable coverage area of snow depth. In contrast to the static retrieval approach, the dynamic retrieval approach avoids efficiently the question that snow depth was overestimated in mountain regions and underestimated in plain regions, so the snow cover and the snow depth are both more real.

Keywords: Snow depth retrieving, Passive microwave remote sensing, dynamical retrieving

 

# Using radar to measure vegetation water stress

*Tim vanEmmerik[1], Susan Steele-Dunne[1], Nick van de Giesen[1]

1. Water Resources Section, Delft University of Technology, The Netherlands

Vegetation water stress significantly affects agricultural and tropical forest canopies. Water shortages in crops influence plant water dynamics, reduces primary production and might eventually lead to plant death. Tropical forests are essential part of global carbon and water cycle. Continuing drying of e.g. the Amazon rainforest might accelerate climate change through carbon losses and changing land surface energy balances.

In addition to ground measurements, various studies have reported observations of plant water stress using active microwave remote sensing. For example, statistical significant variations in radar backscatter were shown to coincide with the onset of water stress over West Africa [1]. Others were able to link radar backscatter time series over the Amazon to the heavy 2005 drought [2].

Additional in situ measurements in agricultural and tropical forest canopies allow further exploration of the full potential of water stress detection using radar. Novel ground measurements techniques have been used to detect and quantify the effects of water stress in various types of plant canopies [3,4], increasing the understanding of how hydrological and plant physiological signatures of water stress affect radar backscatter. Recent efforts have focused on linking these measurements to radar backscatter time series [5].

This presentation aims to present a journey across scales with respect to vegetation water stress. Measurements of changing plant physiological dynamics on leaf and plant levels are linked to radar backscatter on field and forest scales. We aim to demonstrate new insights obtained using field measurements, and highlight the potential of vegetation water stress detection using radar remote sensing.

**References**

[1]. Friesen, Jan, Susan C. Steele-Dunne, and Nick van de Giesen. "Diurnal differences in global ERS scatterometer backscatter observations of the land surface." *IEEE Transactions on Geoscience and Remote Sensing* 50.7 (2012): 2595-2602.

[2]. Frolking, Steve, et al. "Tropical forest backscatter anomaly evident in SeaWinds scatterometer morning overpass data during 2005 drought in Amazonia." *Remote Sensing of Environment* 115.3 (2011): 897-907.

[3]. van Emmerik, Tim, et al. "A comparison between leaf dielectric properties of stressed and unstressed tomato plants." *Geoscience and Remote Sensing Symposium (IGARSS), 2015 IEEE International*. IEEE, 2015.

[4]. van Emmerik, Tim, et al. "Dielectric Response of Corn Leaves to Water Stress." *IEEE Geoscience and Remote Sensing Letters* 14.1 (2017): 8-12.

 

[5]. van Emmerik, Tim, et al. "Impact of diurnal variation in vegetation water content on radar backscatter from maize during water stress." *IEEE Transactions on Geoscience and Remote Sensing* 53.7 (2015): 3855-3869.

Keywords: vegetation, remote sensing, drought

 

# JAXA super sites 500: a large footprint ecological monitoring project for satellite validation

*Tomoko Akitsu[1], Kenlo Nishida Nasahara[1], Tatsuro Nakaji[2], Toshiya Yoshida[2], Nobuko Saigusa[3], Hideki Kobayashi[4], Masato Hayashi[5], Masahiro Hori[5], Yoshiaki Honda[6]

1. University of Tsukuba, 2. Hokkaido University, 3. National Institute for Environmental Studies, 4. Japan Agency for Marine-Earth Science and Technology, 5. Japan Aerospace Exploration Agency, 6. Chiba University

JAXA super sites 500 is a large footprint ecological monitoring project for satellite validation. This project has been started from 2013. Its objective is to obtain representing values of leaf area index (LAI), above ground biomass (AGB), and fraction of absorbed photosynthetically active radiation (fAPAR) within the 500 m ×500 m scale, particularly for validation of the ecological products derived by the Global Change Observation Mission-Climate (GCOM-C) satellite, which will be launched in 2017.

LAI, AGB, and fAPAR are essential information for studies of vegetation productivity and carbon cycle. Therefore, these accurate datasets on global and regional scales are needed to be derived by satellite remote sensing. Generally, these datasets have been produced in a satellite sensor's moderate resolution such as 0.25 km, 0.5 km, or 1 km. To assess their accuracy, in-situ data measured within such spatial resolution is desired. However, such data are rarely available. Accordingly, in previous researches, in-situ data was measured within a smaller area such as 100 m ×100 m and then scaled up to the satellite resolution using higher-resolution imagery. In another case, assuming the larger area was covered with homogeneous vegetation, the in-situ data was directly scaled up to the satellite resolution. However, such scaled-up data includes influences caused by micro-topography and a mixture of different land covers. Thus, the LAI, AGB, and fAPAR products of such satellite sensor's resolution have been difficult to validate.

In order to overcome this difficulty, we initiated a "JAXA Super Sites 500" project. We have established in-situ observation sites on some typical forest types in East Asia, from temperate to cool ecosystems: deciduous needle-leaf forest (DNF), evergreen needle-leaf forest (ENF), and deciduous broad-leaf forest (DBF). Each site has 500 m ×500 m square research plot in flat topography area. We had carried out pilot studies on each site, and will start full-fledged observations after launching of GCOM-C.

The purpose of this study is to compare their observation methods and sampling designs within this scale, and to evaluate the quality of the in-situ data. Basically, we set five 400 m length parallel line-transects at 100 m intervals in each site. LAI and AGB were measured along these lines. Canopy LAI was measured by three methods: It was measured at 20 m intervals on each line by using LAI-2200/LAI-2000 (LI-COR, USA) and fish-eye digital camera. It was also measured by using litter trap. Understory LAI was measured by two methods: It was measured at 20 m intervals by using LAI-2200 and by using harvesting method. AGB was measured by two methods: It was measured at several points by using an improved Bitterlich's method. It was also measured within several fixed plots by using a tree census method. Furthermore, we plan to measure fAPAR by using accurate and stable quantum sensors [*Akitsu et al.*, in press].

Keywords: Satellite validation, Large footprint monitoring, Leaf area index, Above ground biomass, Fraction of absorbed photosynthetically active radiation

 

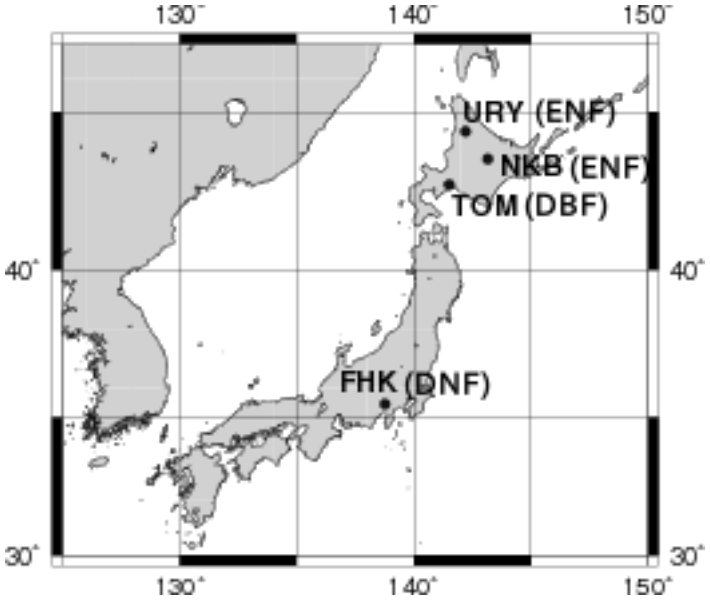


 

# Why Japan's Earth observation has not yet been settled

*Tetsuya Kodama[1]

1. Research Unit I, Research and Development Directorate, Japan Space Exploration Agency

Thirty years have passed since Japan launched its first Earth Obsevation Satellite MOS-1 in 1987.
Due to the introduction of the Information Gathering Satellite Project in 1999, our space program had to suffer heavy staff reduction and budget cuts.
Even after the Basic Space Law was enacted in 2008, the program for the future Earth Observation Satellites is still in a blank state.
In this presentation, a review on the Earth Observation Satellites since the NASDA era and the Task Force Meeting/Remote Sensing Subcommittee (TF) in 2016 together with some proposal for the future program will be presented.

Keywords: Earth Observation Satellite, Space Policy, Decision Making

 

# The potential of GRACE gravimetry to detect fast impoundment of a small reservoir in the upper Yellow River

*Shuang Yi[1], Chunqiao Song[2], Qiuyu Wang[4], Linsong Wang[3], Kosuke Heki[1], Wenke Sun[4]

1. Dept. Natural History Sciences, Faculty of Science, Hokkaido University, 2. Department of Geography, University of California, Los Angeles, Los Angeles, CA90095, United States, 3. Institute of Geophysics and Geomatics, China University of Geosciences, Wuhan, Hubei, China, 4. Key Laboratory of Computational Geodynamics, University of Chinese Academy of Sciences, Beijing 100049, China;

Artificial reservoirs are important indicators of anthropogenic impacts on environments, but their gravity effects have been seldom studied. Here, satellite gravimetry Gravity Recovery and Climate Experiment (GRACE) is utilized to detect the gravity effect of the Longyangxia Reservoir (LR) situated in the upper stream of the Yellow River. Heavy precipitation in the summer of 2005 caused the LR water storage to increase 37.9 m in height or 13.0 Gt in mass. Three different GRACE solutions from CSR, GFZ and JPL and three different filters (an anisotropic decorrelation filter DDK4, Gaussian filter and a decorrelation filter) are compared here. In this case, CSR solutions have the highest signal-noise-ratio and DDK4 shows the best ability to reveal the expected gravity signals. We obtained 109 combinations of inundation area measurements from satellite imagery and water level changes from laser altimetry and in situ observations to derive the area-height ratios in the LR, which agrees well with an alternative method based on the digital elevation model. After removing simulated gravity signals caused by mass changes in the LR, the root mean square of GRACE series in the LR is reduced by 31.1%. If the residuals are totally attributed to GRACE errors, the standard deviation of GRACE observation in this study spot is estimated to be 3.1 cm. With an area of 383 $km^2$, the Longyangxia Reservoir is the smallest signal source reported to be detected by GRACE.

Keywords: GRACE, space gravimetry, gravity of reservoirs, time-varying gravity, reservoir impoundment

 

# Remotely sensed global distribution of debris thermal resistance on glaciers

*Orie Sasaki[1], Yukiko Hirabayashi[2], Shinjiro Kanae[1]

1. Tokyo Institute of Technology, 2. The University of Tokyo

Supraglacial debris is commonly found in high relief mountains and affects glacier melting rate by altering surface reflectivity and conductive heat flux. Several researches therefore developed local glacier models that reflect debris effects. However, there is no global glacier model that includes debris effects in glacier melting process due to limited information about spatial distribution and thermal properties of debris. Here, we present a global distribution data of debris thermal resistance to account for debris effects in global glacier models. We calculated thermal resistance of debris layer at 90m horizontal resolution on a global scale by utilizing ASTER and CERES satellite products in conjunction with meteorological data, excluding Greenland and Antarctica. Result indicated that 16.8% of total glacier area was covered by supraglacial debris, and regional differences are apparent from region to region. When we classified debris into thin debris and thick debris, it was found that thick debris-covered area was larger than thin debris-covered area, with the exception of Svalbard and Scandinavia. Moreover, we assess the possible uncertainties and limitation of our methodology. Although the uncertainties is relatively high, our estimation provides a necessary basis to calculate the debris effects on glaciers on a global scale, which may refine future predictions of glacier meltwater and its contribution to regional water availability and global sea-level change.

Keywords: debris-covered glacier, thermal resistance

 

# Cirrus optical properties analysis based on EarthCARE observation

*Seiko Takagi[1], Makiko Hashimoto[2]

1. Tokai University, Research and Information Center, 2. JAXA

Cirrus clouds play an important role in the energy budget of the Earth-atmosphere system by their effects on the transfer of radiative energy through the atmosphere. Low clouds have a cooling effect on solar radiation by scattering. On the other hand, the high thin cirrus clouds scatter a small amount of solar radiation and absorb a large quantity of outgoing long-wave radiation from the Earth and its atmosphere. The overall effect of the high thin cirrus clouds is heating on the Earth-atmosphere system.
Cirrus clouds are prominent and yet uncertain components in weather and climate studies because of high location and composed of almost exclusively nonspherical ice crystal of various shapes, such as bullet rosetts, plates, and columns. Progress in numerical model of climate change prediction require improved representations of cloud processes and decreased uncertainties in parameterizations of cloud radiation interactions. Cloud parameterizations in numerical climate models need to define the temporal and spatial distributions of high cloud optical properties. EarthCARE (Earth Clouds, Aerosols and Radiation Explorer) is one of the future Earth observation joint mission of Japanese (JAXA) - European (ESA). EarthCARE satellite aims at understanding of the role that clouds and aerosols play in reflecting incident solar radiation back into space and trapping infrared radiation emitted from the surface in order to improve the numerical climate prediction models. The satellite payload is composed of four instruments; an Atmospheric backscatter Lidar (ATLID), a Cloud Profiling Rader (CPR), a Multi-Spectral Imager (MSI), and a Broad-Band Radiometer (BBR). The EarthCARE orbit is sun-synchronous with an altitude of around 393 km and 14:00 mean local time of the descending node. The MSI will provide Earth images over a swarth width of 150 km with a spatial resolution of 500×500 m in 7 spectral bands; one visible (0.67 um), one near infrared (0.865 um) and two shortwave infrared (1.65, 2.21 um) channels capturing reflected solar right on the day-side of the orbit, and three thermal infrared (8.80 10.80, 12.00 um) channels measuring the emitted thermal radiation from the Earth.
We develop an algorithm to derive cirrus clouds optical properties from MSI Level 2 radiance data as a research product of EarthCARE project. In this study, we modified MWP (Multi-wavelength and multi-pixel) method [M. Hashimoto et al., in revision] to derive cirrus clouds optical properties and operation tests of modified algorithm were performed in using MODIS/Aqua radiance data for the first time.

Keywords: EarthCARE, cirrus

 